Received May 10, 2018, accepted July 30, 2018, date of publication August 16, 2018, date of current version September 7, 2018.

Digital Object Identifier 10.1109/ACCESS.2018.2865792

Determination of the Spatial Pattern of Wave Directions in the Inhomogeneous Coastal Ocean by Marine Radar Image Sequences

DONG-JIING DOONG[1], LI-CHUNG WU[2], AND JIAN-WU LAI[3]

[1]Department of Hydraulic and Ocean Engineering, National Cheng Kung University, Tainan 70101, Taiwan
[2]Coastal Ocean Monitoring Center, National Cheng Kung University, Tainan 70101, Taiwan
[3]Taiwan Ocean Research Institute, National Applied Research Laboratories, Kaohsiung 80143, Taiwan

Corresponding author: Li-Chung Wu (jack18@mail.ncku.edu.tw)

This work was supported by the Ministry of Science and Technology of Taiwan under Grant MOST 106-2628-E-006-008-MY3 and Grant MOST 106-2221-E-006-112.

ABSTRACT Remotely sensed images of the ocean are a useful tool for revealing wave direction information in the spatial domain. Considering wave inhomogeneities in a coastal area, this paper addresses issues concerning the analysis of local wave directions using a simultaneous time series of *X*-band radar echo intensities. The method employed to analyze the directional wave information in our paper is based on a cross-spectral analysis of radar echo intensity time series from several neighboring locations constituting a spatial array within a small area. Compared with simultaneous sea surface elevation records, which have demonstrated their efficacy for estimating directional wave information, the spatial wave features present in radar image sequences are more sensitive to environmental factors and image noise. To confirm the practicality of this approach, we examined the relationship between the wave directions estimated from the *X*-band radar and moored buoy data. Most mean wave directions and dominant wave directions estimated from the radar images are consistent with the buoy results. In most cases, the differences between the radar and buoy wave directions are within $\pm 30^{\circ}$. We also present a radar image case with an obvious refracted wave pattern. The results estimated from this image case demonstrate the feasibility of determining the spatial pattern of wave directions from a highly inhomogeneous wave field.

INDEX TERMS Local wave direction, pixel array, X-band radar.

I. INTRODUCTION

The wave direction is one of the most important parameters to quantify when examining the physical characteristics of ocean surface waves. Some studies have shown that the probability of the formation of large-amplitude waves strongly depends on the directional properties of waves [1]. The wave energy travels in the same direction as the wave if current-induced refraction is neglected. As waves approach the shoreline, both the wave energy and the momentum are conveyed in the wave direction. Wave direction data are also necessary to predict the responses of ships to sea conditions as the spectra of their motions are obtained from directional wave spectra. In summary, wave direction data constitute necessary inputs for the correct design of solutions to various ocean and coastal engineering problems.

In situ wave gauges and moored buoys are frequently used to measure the directional spreading of wave energy by analyzing the directional wave spectrum. After estimating the cross-spectra among different wave sensors, the directional spectrum is determined by inverting the relationship between the cross-spectra and the directional spectrum. To obtain complete directional information, a wave sensor array, which comprises 3 to 10 wave gauges, is typically necessary [2]. In theory, the presence of additional wave gauges permits more complete wave directional information to be acquired. However, more wave gauges mean higher costs and difficulties with observation.

Most in situ wave measurement techniques are designed to record ocean wave information in the time domain; it is not as easy to collect wave information in the space domain from a small amount of in situ measurement instruments. An ocean wave field obtained by remote sensing techniques is a useful way to present wave features in the space domain. Due to the modulation of backscattered microwave power by long

ocean waves through Bragg-scattering waves as well as the effects of shadowing by the wave crest [3], [4], the spatial ocean wave pattern is present in images from many different frequency bands of electromagnetic waves.

Given the continuous development of remote sensing platforms, many different types of ocean remotely sensed images are capable of presenting wave patterns. Satellite-based remote sensing instruments provide a large-scale view of wave patterns in the spatial domain. Compared with remote sensing by aircraft or satellites, the advantage of land-based radar technology lies in its ability to continuously monitor wave patterns. Nautical X-band radar, which is normally used to detect the coastline and obstacles on the sea surface on board a ship, is currently one of the most popular tools for ocean remote sensing. Different studies have confirmed a mechanism for imaging sea surface wind waves patterns by means of X-band radar [6]. Based on the principle of sea surface wave imaging, the feasibility of ocean wave observation has also been demonstrated [7]. Although the observation area of land-based X-band radar is smaller than those of satellites or aircraft, continuous measurements using land-based radar provide spatiotemporal information on ocean waves that avoids ambiguity in estimating wave propagation directions [8]. Additionally, ocean wave imaging from a fixed radar station is free of the velocity bunching mechanism that smears out the wave pattern when the airborne flight direction is parallel to the wave direction [9].

To reveal wave features from ocean remotely sensed images, different methods have been proposed to analyze the image spectrum. Some studies have comprehensively reviewed recent studies of ocean information extraction from X-band radar images [10]. The Fourier transform algorithm, which is one of the most commonly used methods for identifying periodic components in stationary data, has often been applied in the past to calculate the image spectrum [5]. Accordingly, some studies have demonstrated the feasibility of estimating the wave direction from X-band radar images based on the Fourier transform algorithm [11]. However, spatial inhomogeneity must be treated carefully when investigating waves near the shore. For a wave traveling over irregular bottom depths, the change in the wave speed along the wave crest implies that the wave changes direction locally. Consequently, for three-dimensional image spectrum analysis using the Fourier transform algorithm, the assumptions of homogeneity within the analyzed spatial area and temporal stationarity within the analyzed duration are necessary. Because the duration of each radar image sequence in our study is approximately 183 s, wave features within this short duration can be regarded as stationary. However, a homogeneous wave field in the coastal area is nearly impossible due to the influence of the shallow water topography. To overcome the issues associated with an inhomogeneous wave field, some studies determined the spatial maps of local wavenumber vectors using the phase of complex-valued one-component images [12]. In contrast to the majority of studies, which analyzed whole radar images in the first step, our study tried to determine the local wave information from the image intensities of only several pixels within a local area. Some studies noted that radar data from a local area reduce inhomogeneous effects due to small grazing angle shadowing. Once the shadow effect is suppressed, there is no need to use a modulation transfer function to amend the directional spectrum [13]. Some studies have further shown that in situ sensor arrays are capable of providing the local directional spectrum [14], and the degree of directional resolution depends on the number of sensors and their spacing. However, measurements of the wave directionality using in situ senor arrays are laborious and costly. Radar image sequences provide a potential and inexpensive approach to estimate the spatial pattern of wave directions within a sea area of several square kilometers. We are able to treat sea surface image sequences that have a size of M $\times$ N pixels in the spatial domain and T samples in the time domain as an array with M $\times$ N sensors that records T samples simultaneously. However, marine radar systems record the echo intensity from the sea surface rather than recording the actual water displacement. Although radar echoes do not exactly represent the sea surface elevation profile, the qualitative features of the ocean wave steepness are present in radar images due to tilt modulation. Phase information of longer ocean waves in the spatial domain may also be roughly estimated due to the shadowing effect of radar imaging. In summary, marine radar image sequences may be a useful tool for revealing local wave directions from highly inhomogeneous wave fields. However, this issue has received little attention. Therefore, this study attempted to confirm the feasibility of estimating local wave directional features from sea surface radar image sequences using a method that was applied to data from an in situ sensor array. In the subsequent sections, we will demonstrate the entire image processing procedure and discuss its practicability using coastal radar images.

II. THEORETICAL PRELIMINARIES

Tracking wave crest signatures on a spatial sea surface image is the most direct way to estimate the wave direction. Some studies have estimated the wave direction by extracting linear wave crest signatures from video images under the assumption that the wave direction is perpendicular to elongated wave crests [15]. However, clear and sufficiently long wave crest signatures in the image are necessary for image processing. Radar imaging mechanisms are related to many different dependencies and modulations [11], and clear and long wave crest signatures are not always available for all radar images.

Other studies have estimated the two-dimensional wavenumber spectrum from a single spatial image using the discrete Fourier transform algorithm and determined the wave direction θ based on the relationship between the wavenumbers along the x and y directions (k_x and k_y, respectively):

$$\theta = \tan^{-1}\left(k_y/k_x\right) \tag{1}$$

To avoid ambiguity in the wave propagation direction, successive images were analyzed by the Fourier transform method [8]. Whether single images or image sequences are used, the assumption of spatial homogeneity within the spatial domain is necessary. It is feasible to apply some theories, e.g., the wavelet transform theory, to analyze local wave information from the inhomogeneous wave field. However, local wave information results from the wavelet transform method are still limited by the mother wavelet function, image size and spatial resolution [16].

In contrast to methods used to estimate the image spectrum from full frame images, methods for analyzing the directional spectrum from in situ sensor array records focus only on the wave features within a local area. Most in situ directional wave measurements consist of a time series of various wave kinematical quantities, e.g., surface elevation, water velocity, surface slope, and dynamic pressure [17]. Cross-spectra are estimated between the simultaneous wave records from different in situ sensors. To estimate ocean wavenumbers, some studies developed methods based on the cross-spectral correlations between different intensity time series from a subset of image pixels [18], [19]. The wave direction can be estimated by wavenumbers using (1) directly. The method to analyze directional wave information in our study is also based on cross-spectral analysis. The directional wave spectrum, which presents directional features of different wave components, is estimated based on the known mathematical relationship between the directional spectrum and the cross-spectra. Notably, the radar echo intensity of the sea surface is not the sea surface elevation; the relationship between them is nonlinear. Until now, there has been no deterministic model that describes the complete quantitative relationship between the radar echo intensity and sea surface elevation. However, the radar echo intensity is increased near the wave crest based on the radar imaging mechanisms of tilt, hydrodynamic and orbital modulations. Low echo intensities are related to the wave trough based on the imaging mechanism of the shadowing modulation. Due to the joint effects of the low grazing observational angle of land-based radar and the hydrodynamic modulation of ocean waves, high radar returns appear at the front faces of traveling waves instead of the crests of ocean waves. From a geometric perspective, the distances between the real wave crest and high echo signatures on radar images should be close within a small spatial area. In other words, the shapes of cross-spectra analyzed from spatiotemporal radar data should be similar to the shapes of cross-spectra analyzed from simultaneous and co-located in situ data. To analyze the directional wave features from radar image sequences, we attempt to use a radar echo intensity time series from several neighboring locations as a spatial array within a small area. However, in addition to sea surface waves, other environmental factors also influence the radar images. Filtering is required because of the nonlinearity of radar images of the sea surface waves [12]. To avoid the influence of noise on the estimation of wave direction, a filter based on the linear wave dispersion relation was applied to process all the radar images in our study.

A directional spectrum provides the distribution of the radar echo intensity variance as a function of both the angular frequency f and the direction θ. The directional spectrum $I(f,\theta)$ is written as:

$$I(f,\theta) = I(f)\, D(f,\theta) \tag{2}$$

where $I(f)$ is the frequency spectrum of the radar echo intensity, and $D(f,\theta)$ is the directional distribution. The directional spectrum is estimated if the wave properties are simultaneously recorded for a large number of samples. As shown in [20], the general relationship between the cross-spectrum $\Phi_{mn}(f)$ for a pair of wave properties and the directional spectrum $I(f,\theta)$ is expressed as:

$$\begin{aligned}\Phi_{mn}(f) = \int_0^{2\pi} & H_m(f,\theta)\, H_n^*(f,\theta) \\ & \times \{\cos[k(x_{mn}\cos\theta + y_{mn}\sin\theta)] \\ & - i\sin[k(x_{mn}\cos\theta + y_{mn}\sin\theta)]\} \times I(f,\theta)\, d\theta\end{aligned} \tag{3}$$

where $\Phi_{mn}(f)$ is the cross-spectrum between the m- and n-th records, k is the wavenumber, $\vec{x}_m$ and $\vec{x}_n$ are the respective location vectors (x_m, y_m) and (x_n, y_n) inside the image pixel array for the m- and n-th records, * is the conjugate complex, and $H_m(f,\theta)$ is the transfer function from the water surface elevation to the m-th wave property. Until now, no theoretical transfer function between the water surface elevation and radar echo intensity has been developed. As discussed above, the shapes of spectra analyzed from radar data should be similar to the spectral shapes analyzed from in situ data. However, the energy density of radar cross-spectra is not equal to the wave energy. Given that we focus only on the issue of wave direction estimation, the values of both $H_m(f,\theta)$ and $H_n(f,\theta)$ are set as 1 in this study.

Theoretically, Equation (3) determines the directional spectrum if the cross-power spectra are known for an infinite number of pairs of corresponding location-dependent m and n values. Considering the practical application of radar data, only a limited number of wave properties are measured at a limited number of locations within a small sea area. To determine the directional spectrum from a limited number of wave properties, a specialized formulation is introduced to obtain a unique function representing the directional spectrum. Certain higher-resolution techniques, such as maximum entropy methods (MEM) and maximum likelihood methods (MLM), have been developed to estimate the directional spectrum from spatial array data [21]. However, the conventional estimation method, which is based on the direct Fourier transform method (DFTM) expansion, is still widely used due to its stability and simplicity. Because the aim of this study is to confirm the feasibility of local wave direction estimation using spatial array echo intensity data rather than discussing which method is the best, we estimate local wave information

from radar image sequences using only the DFTM method:

$$\hat{I}\left(f,\vec{k}\right)=\sum_{m}\sum_{n}\phi_{mn}\left(f\right)\exp\left[i\vec{k}\left(\vec{x}_n-\vec{x}_m\right)\right] \quad (4)$$

The wave direction θ can be estimated by the wavenumber $\vec{k}$ using (1) directly. The wavenumber $\vec{k}$ is related to the angular frequency ω by the dispersion relation that includes the influences of the water depth d and sea surface current $\vec{u}$:

$$\omega=\sqrt{g\left|\vec{k}\right|\tanh\left(\left|\vec{k}\right|d\right)}+\vec{k}\cdot\vec{u} \quad (5)$$

III. DATA SOURCE

The radar image cases in this study were collected from the coastal areas throughout a southern region of Taiwan. Approximately 1,000 image cases were used. Table 1 shows the properties of our radar equipment. The marine radar is horizontally polarized. The radar device is equipped with a 42-rpm antenna, which yields an image sequence sampling rate of 0.7 Hz. We collected 128 continuous radar image sequences over a spatial range of 3,750 m with a grid size of 7.5 m ($\Delta x = \Delta y = 7.5$ m). This means that the nearest distance between two records of radar echo intensity is 7.5 m. The system stores the logarithmically amplified radar backscatter information at a 12-bit image depth. Fig. 1 shows the sea area of this experiment. Wave data that are measured by an in situ moored buoy are used for comparison to confirm the wave direction results estimated from the radar image sequences.

TABLE 1. Properties of our X-band radar equipment.

Operating frequency of radar system	9.4 GHz
Polarization of radar antenna	HH
Spatial resolution of radar image	7.5 m/pixel
Image sequence sampling rate	0.7 Hz

Some studies have proposed different types of pixel position patterns [22]. Because the radar image pixels we used constitute an equally spaced grid, the selected pixels are adopted as a planar uniform pattern. To estimate the wave directions from radar data, we adopt a simple and regular image pixel array. Radar echo intensity records from different image pixels are used to analyze the cross-spectra with each other. Fig. 2 shows the locations of selected echo intensity records. Although this type of planar uniform pattern may not be optimal, it is easy and convenient for analyzing radar data. Because simultaneous radar echo intensity records from a small number of image pixels are used in this study, the wave direction estimation results are influenced by the distances between different selected pixels. To avoid signal aliasing in the spatial domain, the distances between selected pixels should be less than one-half of the wavelength. However, the directional resolution of the directional spectrum increases as the maximum distance between selected pixels increases [23]. The distance between each pair of

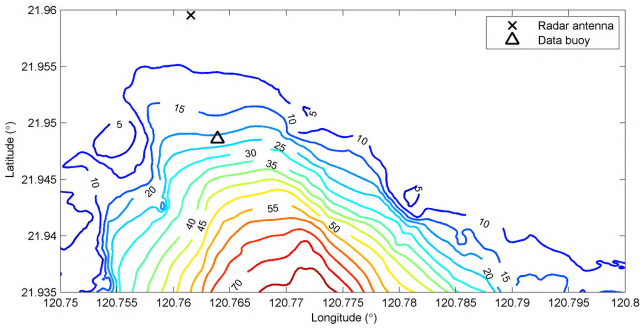

FIGURE 1. Bathymetry of our study site (water depth unit: meters). The distance between the radar antenna and moored buoy is approximately 1 km. The water depth of the moored data buoy is approximately 20 m.

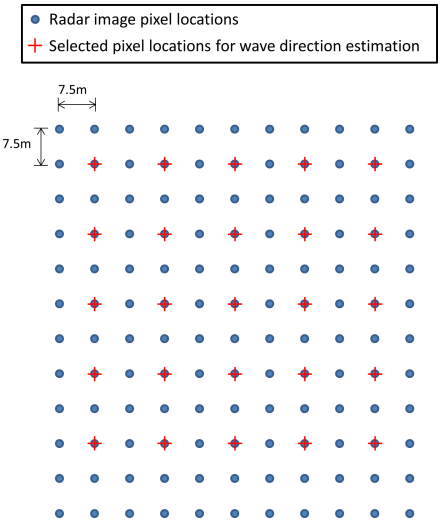

FIGURE 2. Pixel selection for the wave direction estimation. The distance between each pair of two selected pixels is set as 15 m. This distance is roughly one-half of the 4.5-s period waves.

two selected pixels is set as 15 m. This distance is approximately half of the 4.5-s period waves that occur frequently in our study site. Fig. 3 shows one case of a radar image. This wave image, which forms due to the different modulations discussed above, is not equal to the real spatial wave field. However, wave direction features are present in wave patterns in the image. For this reason, some studies have revealed directional wave features using X-band radar images [24].

Before estimating the directional spectrum from radar signals, we separated the wave signal from the noise in the complex spectrum using the dispersion filter. The circles in Fig. 4 show the radar energy densities in the spectral domain. The theoretical dispersion relation is also shown by the three-dimensional contours in Fig. 4 as well. Fig. 4 shows that the energy densities in the lower and higher angular frequency bins deviate from the linear wave dispersion relation. The energy density that deviates from the linear wave dispersion relation is regarded as noise. After filtering out the noise in the spectral domain, we obtained the filtered image sequences by the inverse Fourier transform of the complex spectrum.

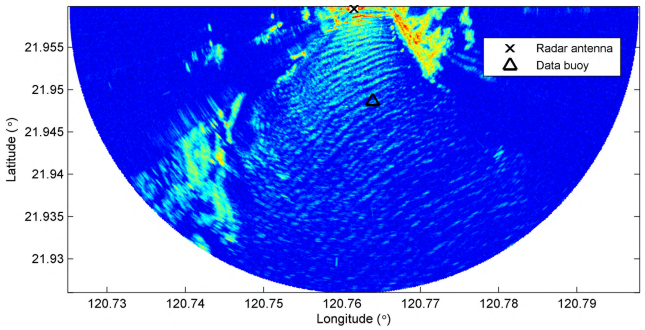

FIGURE 3. One radar image case. Wave crest patterns are formed by the contrast between the radar echo intensities at different pixels.

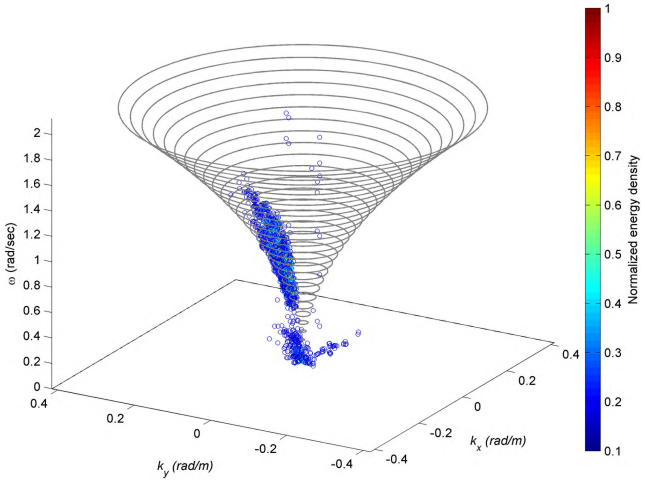

FIGURE 4. Three-dimensional radar image spectrum and theoretical dispersion relation. The normalized energy densities are marked by circles. The theoretical dispersion relation is presented with three-dimensional contours.

Fig. 5 shows the time series of the radar echo intensity before and after filtering. Although most of the radar echo intensity amplitudes decrease after filtering, the filtered waveforms within the time series are more symmetrical than the unfiltered waveforms. To obtain reliable directional wave features, all of our radar image cases are processed using dispersion filtering.

IV. COMPARISON OF THE WAVE DIRECTIONS ESTIMATED FROM RADAR AND BUOY RECORDS

The wave data obtained by the in situ buoy are used to verify the directional results from radar images. We also applied the DFTM to estimate the directional spectrum from the moored buoy data. Unlike the radar echo intensity, the analyzed data from the buoy are composed of wave accelerations, east-west wave slopes, and north-south wave slopes. The sampling rate of these buoy records is 2 Hz. For each case, the duration of data acquisition is 10 minutes, indicating that 1,200 data points will be recorded in each hour. To apply the DFTM to our study, we selected the first 1,024 data points from each case for further analysis.

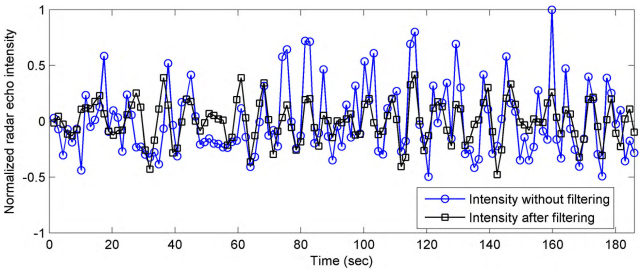

FIGURE 5. Time series of the radar echo intensity of a sea surface image before and after filtering. Both time series are extracted from the same pixel.

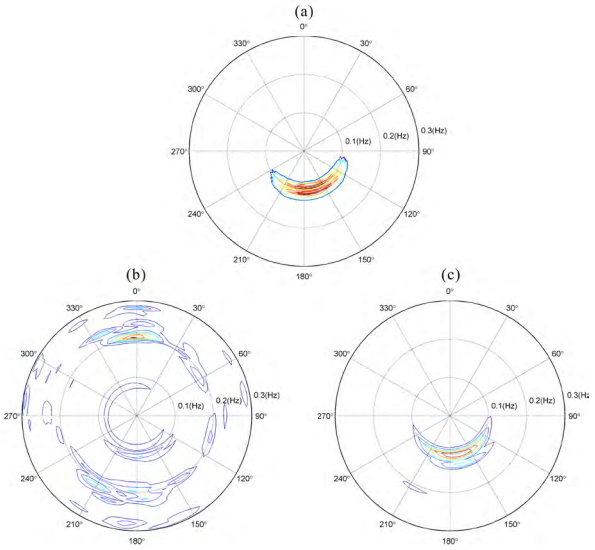

FIGURE 6. One case of the directional spectra estimated from (a) buoy data, (b) radar pixel array data before filtering, and (c) radar pixel array data after filtering. Compared with the spectrum of (b), the directional spectrum from filtered radar signals is more consistent with the directional spectrum from buoy data. The wave height for this case is approximately 1.5 m.

Fig. 6 shows one case consisting of the directional spectra estimated from buoy and radar data. The spectrum of radar data is estimated from the radar echo intensities of one pixel array whose central pixel is at the same location as the moored buoy. The estimated directional spectrum from unfiltered radar signals shows obvious noise at different frequencies and directions. The directional spectrum from the filtered radar signals is more consistent with the directional spectrum from the buoy data. The energy densities from the filtered radar and buoy spectra focus on similar directional bins. However, the features of spectral shapes, e.g., directional spreading, from the radar and buoy results are different. Directional spreading is expressed as [25]:

$$\sigma_{\hat{\theta}}(f) = \sqrt{\int_{-\pi}^{\pi} \left[2\sin\left(0.5\hat{\theta}\right)\right]^2 D\left(\hat{\theta}; f\right) d\hat{\theta}} \qquad (6)$$

where $\hat{\theta}$ is taken relative to the mean wave direction $\bar{\theta}$, and $D\left(\hat{\theta}\right)$ is the function of the directional

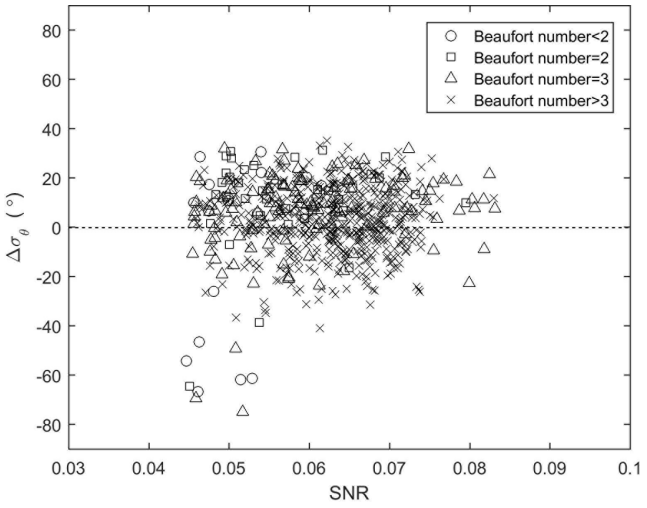

FIGURE 7. Directional spreading at the peak frequency estimated from the radar and buoy directional spectra. Most of the directional spreading values estimated from radar data are lower than the buoy results.

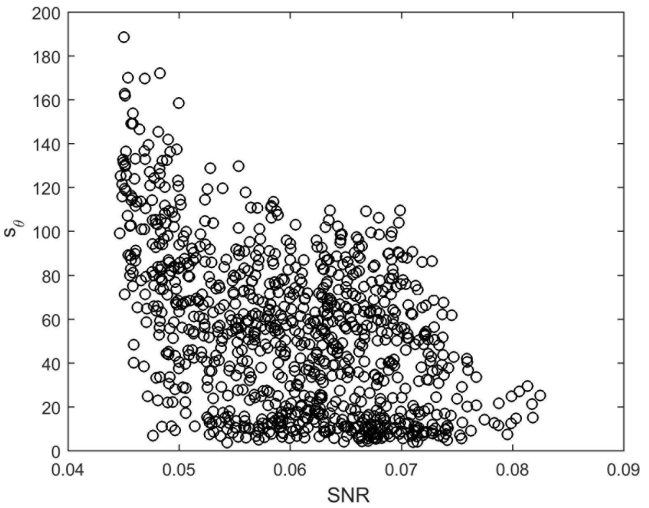

FIGURE 8. The relationship between the SNR and S_θ.

distribution:

$$\bar{\theta} = \tan^{-1}[\int \sin\theta \cdot \hat{I}(f,\theta)\, dfd\theta \Big/ \times \int \cos\theta \cdot \hat{I}(f,\theta)\, dfd\theta] \quad (7)$$

$$D\left(\hat{\theta}\right) = \hat{I}\left(f,\hat{\theta}\right) \Big/ \hat{I}(f) \quad (8)$$

Fig. 7 shows a comparison of the directional spreading results $\sigma_{\hat{\theta}}(f_p)$ at the peak frequency f_p estimated from the radar and buoy directional spectra. Most of the differences between the radar and buoy results are within 30°. As mentioned above, the radar echo intensities from the image sequences are used to estimate the directional spectrum in this study. Imaged wave patterns exhibit different dependences and modulations. Although a dispersion filter is applied to improve the quality of the directional spectra, wave patterns imaged from radar echo intensities still do not absolutely represent real waves. We also notice that the differences in the estimated directional spreading can exceed 60° in a few of the cases. Fig. 7 shows the relationship between the wind conditions and the directional spreading results. The wind data are measured by an anemometer on the moored buoy. Our in situ wind speed data are classified according to the Beaufort scale. In theory, the poor directional spreading results should be caused by low wind conditions, which cannot induce a rough sea surface. Furthermore, radar backscattering by the rough sea surface at low grazing angles is a key radar imaging mechanism. However, Fig. 7 shows a weak relationship between the poor directional spreading results and low wind conditions. Because our study site is close to an ocean bay, complicated landforms influence the wind conditions. This influence is likely responsible for the lack of a clear relationship between the wind conditions and the directional spreading accuracy. Additionally, the difference between the radar azimuth and wave direction is a significant factor influencing the estimation of directional spreading. Some studies demonstrated that the wave parameters estimated from marine radar images exhibit a strong dependency on both the range and the azimuth of the observations; they also presented evidence demonstrating that the signal-to-noise ratio (SNR) in the radar image spectrum is influenced by the radar range and azimuth [26]. Fig. 7 illustrates that the poor directional spreading estimates are obviously related to a lower SNR, which is determined by separating the different spectral components before implementing the dispersion filter [7]. A low SNR represents weak wave signals from sea surface images. A directional spectrum estimated from radar images with weak wave signals cannot produce accurate directional spreading results.

We further investigated the quality of the estimated directional results based on the parameter S_θ, which is the standard deviation of $\Delta\theta(f_i)$:

$$\Delta\theta(f_i) = \theta_p(f_i) - \theta_p(f_{i-1}) \quad (9)$$

where θ_p is the most energetic direction of the directional distribution in the frequency bin f_i from the directional spectrum. For spectra with a narrow energy density distribution, the representation of the wave direction is clearer than that for spectra with a wide energy density distribution. Because the main energy densities of narrow directional spectra are concentrated within small ranges of frequency and directional domains, the value of S_θ is smaller. In contrast, a high value of S_θ corresponds to a scattered energy density distribution. As shown in Fig. 8, the cases of higher values of S_θ also feature lower SNR values. Thus, the scattered energy density distributions of directional spectra are from the radar image cases with low SNR values. We can confirm that the unstable results of directional information are from the cases of weak wave signals.

The wave directions estimated from radar data are more stable than the results estimated from directional spreading data. Fig. 9 shows the differences in the wave directions

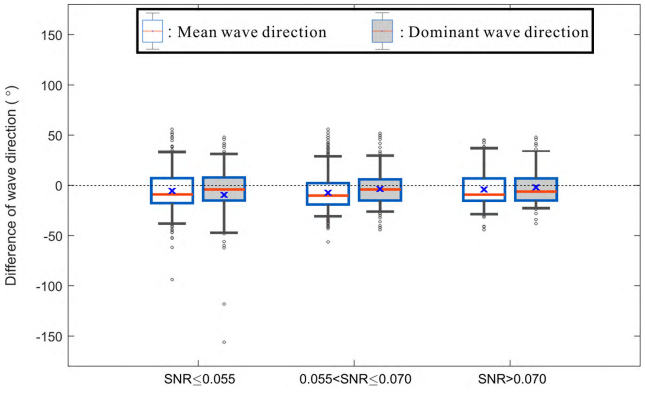

FIGURE 9. Differences in the wave directions. The top and bottom of each box are the 25th and 75th percentiles of the samples, respectively. The line in the middle of each box is the sample median. The cross mark near the middle line is the sample mean. The upper and lower whiskers indicate the 5th and 95th percentiles of the samples, respectively.

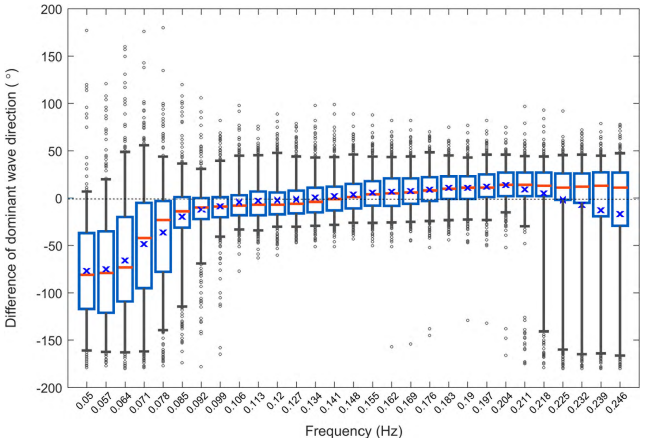

FIGURE 10. Differences in the dominant wave directions at different frequency bins. The definitions of different markers are the same as those in Fig. 9. Differences between estimated dominant wave directions from radar and buoy data are obvious at lower and higher frequency bins.

estimated from radar and buoy data. Different statistical descriptions of wave directions are obtained from the directional spectra. The two most well-known directional statistics, the dominant wave direction and mean wave direction, are discussed in our study. The definition of the mean wave direction is expressed in (7). In most cases, the differences between the radar- and buoy-derived mean wave directions are within $\pm 30°$. The dominant wave direction is defined as the direction of the most energetic wave in the spectrum according to the World Meteorological Organization. The comparison of the dominant wave directions is similar to that of the mean wave directions. Fig. 9 also shows the influences of the SNR on the estimated wave direction results. From the cases with a lower SNR, more inaccurate wave direction estimations are revealed. Thus, the quality of the estimated wave directions from radar data can be confirmed using the SNR from the directional spectrum. Fig. 9 presents the estimated wave direction results from the whole frequency domain. We further discuss the estimated wave directions from different wave frequency components in Fig. 10. Given various sampling rates and data lengths, the frequency bins of the spectra from the radar and buoy data are different. For the comparison in Fig. 10, the frequency bins are determined based on the radar spectrum. The frequency bins from the buoy are changed to the radar frequency bins using nearest neighbor interpolation. Fig. 10 shows that the differences between the dominant wave directions estimated from radar and buoy data are obvious at lower and higher frequency bins. Most of the dominant wave directions from radar and buoy data are close within the frequency range of [0.099, 0.211] Hz. Because the waves follow the buoy, the buoy cannot sense the slopes of waves whose wavelengths are less than twice the diameter of the buoy. The diameter of the buoy used in this study is 2.5 m. Thus, the buoy measures waves that are larger than at least 5 m in length. According to the wave dispersion relation, 5-m waves are equal to a 1.8-s period in deep water. As discussed above, the distance of the radar pixel array is 15 m, which is roughly one-half of the 4.5-s period waves. As a result, waves that are shorter than 4.5 s and whose wave frequencies are larger than 0.22 Hz should be aliased after being sampling by the pixel array. Conversely, the accuracies of the estimated wave directions from radar data are also influenced by longer waves. As discussed above, the wave patterns on the radar image are related to different modulations and shadowing effects. For longer wave patterns, the shadowed area should be larger for a low grazing angle of observation. Based on the definition of geometric shadowing, the signal received from the shadowed area is at or close to the noise level. If the distance between the selected pixels is less than the length of the shadowed area, the cross-spectrum estimated among the time series from different image pixels does not effectively represent the characteristics of real ocean waves. As a result, the estimate of the directional spectrum is often biased by noises and errors associated with cross-power spectra. Although we separated the wave signals from the noise using the dispersion filter, inaccurate wave direction estimates from shorter and longer waves remain unavoidable. In summary, the dominant wave directions estimated from the specified frequencies of radar directional spectra demonstrate better agreement with the buoy results at the frequency bins within [0.099, 0.211] Hz, which is approximately equal to a period of 5-10 s.

Additionally, the maximal tidal range is approximately 1.5 m in our study area. As shown in (5), the wave number estimation is based on the wave dispersion relation. The influence of the tide changes with the water depth continuously. This affects the estimation of the spectrum, especially at low-frequency bins. Moreover, sea surface currents affect the estimation of the spectrum obviously at high-frequency bins. The current speeds in our study site are mostly less than 0.3 m/s. Because simultaneous current data are often unavailable, we ignore their influences in (5). As a result, the accuracies of our estimated directional spectra at higher

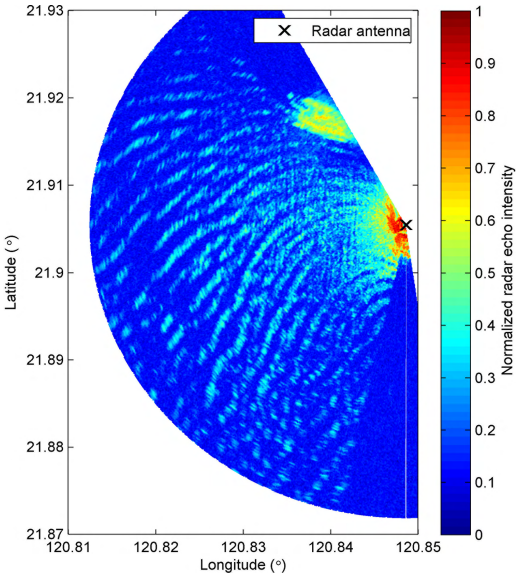

FIGURE 11. A radar image of a refracted wave pattern. Due to the shadowing of the land obstacle near the radar antenna, clear wave patterns on the radar image are present only within the azimuth of 190-350°.

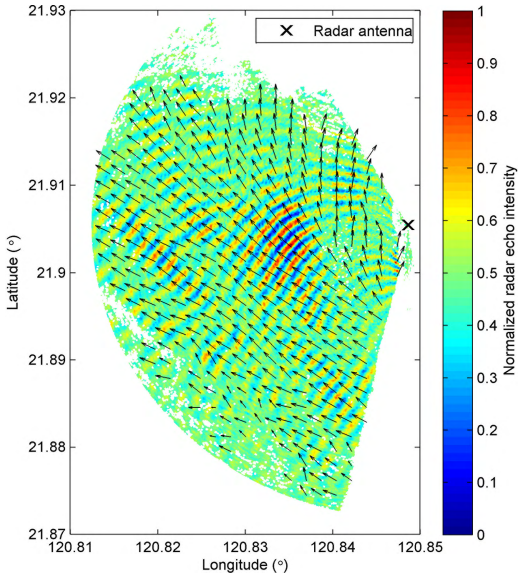

FIGURE 12. Estimates of the spatially dominant wave directions from refracted wave patterns. The arrows present the estimated dominant wave direction. The distance between neighboring wave direction vectors shown in this figure is 187.5 m, which is equal to 25 image pixels.

and lower frequency bins are affected due to the lack of simultaneous tide and current data.

V. CASE STUDY OF A SIGNIFICANT INHOMOGENEOUS WAVE FIELD

After confirming the wave direction relationship between radar and buoy records, we focus on local wave direction estimation in the spatial domain. A radar image case presenting highly inhomogeneous wave patterns is shown in Fig. 11. Note that the location of this radar image is not the same as the case shown in Fig. 3. For the radar image case in Fig. 11, a typhoon was located to the south in our radar observation area. Longer waves induced by the typhoon propagated roughly from the southeastern corner of the radar observation area to the northwestern corner. However, waves were refracted due to the shallow water area near the shore. As a result, the patterns of long crested waves are curved. As discussed above, the directional spreading results estimated from the radar image pixel array data are not stable. Here, we present only the wave direction results.

Based on the wave patterns in Fig. 11, waves from different frequency components are combined together. To show the wave patterns clearly, we decompose the original wave image signals into different mono-component signals. Image decomposition methods based on the Fourier transform method and its inverse transform in the time domain were implemented in our study [27], [28]. The image in Fig. 12 shows the decomposed wave patterns. According to the wave dispersion relation, longer period waves are more sensitive to the sea bed and are refracted due to the change in water depth. Patterns of 8-s-period waves are presented in Fig. 12. Based on the results in Fig. 10, the wave direction estimation with 8-s waves using the radar data is reliable.

Because a clear wave pattern on the radar image is the key to accurately estimating the wave direction, we filtered out the echo intensities with very unclear patterns before the wave estimation. To define unclear wave patterns, the SNR at different locations within the image is evaluated:

$$R_{SN}(x,y) = \int_{f\in f_s} F(x,y,f)\,\mathrm{d}f \Big/ \int_{f\in f_n} F(x,y,f)\,\mathrm{d}f \qquad (10)$$

where $R_{SN}(x,y)$ is the SNR, $F(x,y,f)$ is the frequency spectrum of the radar echo intensity at the location (x,y), f_s denotes the frequency bins of wind-generated waves that are defined within 1–0.03 Hz, and f_n are the frequency bins that are outside of the frequency range of wind-generated waves. For our image case, we filter out the echo intensity at location (x,y), whose $R_{SN}(x,y)$ is less than 15% of the maximal $R_{SN}(x,y)$ within the whole spatial domain. As shown in Fig. 12, most of the unclear wave patterns that are far from the radar antenna have been filtered out. The arrows in Fig. 12 represent the estimated dominant wave directions within the radar observation area. Some basic features of the wave propagation into the shore are visible. The directions of the arrows are almost perpendicular to the wave crest patterns. Most of the local wave directions are southeast-northwest. However, the local wave directions close to the radar antenna are obviously different. South and southeast wave directions are frequently presented in the sea area close to the radar antenna. However, a few unreasonable wave direction results are identified based on the neighboring wave directions. These unreasonable wave direction results are located in areas of slightly unclear wave patterns, which were not filtered out from Fig. 12. Fig. 13 shows a histogram of the estimated wave direction results from Fig. 12. Although most of the wave

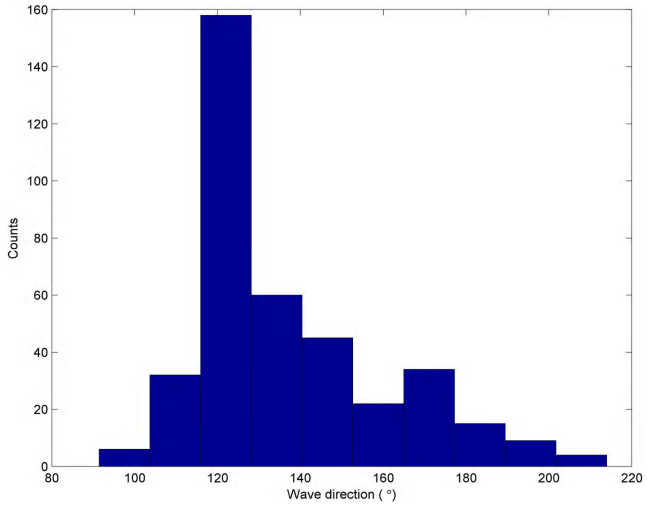

FIGURE 13. Histogram of wave directions within the radar observation area. Some directions are situated far from the directions that occur most frequently.

directions are approximately 130°, some directions that lie far outside this range cannot be ignored. Our results show that the nearshore wave directions are much different than the offshore wave directions. For inhomogeneous wave cases, a single wave direction is unable to represent real wave features.

VI. CONCLUSIONS

The issue of wave direction has received less attention in previous studies than the wave height and wave period. However, the significance of the wave direction for different applications in the ocean environment, such as sailing safety, engineering design, disaster prevention and coastal management, must not be ignored.

Many previous studies have demonstrated the advantages of ocean remotely sensed images as a tool to reveal wave direction information in the space domain. Most of these studies focused on homogeneous wave direction analysis from the image spectrum, and only one representative direction was obtained from the whole image; however, this technique is inappropriate for an inhomogeneous wave field, which is a common occurrence in the coastal ocean. Spatiotemporal wave records are the most common data with which to estimate the local characteristics of directional surface waves. An analysis of the simultaneous records of sea surface echo intensities from a selected radar image pixel array is proposed to reveal the inhomogeneous wave directions. Wave data observed by an in situ buoy are used to verify the directional results from radar images. Most mean wave directions and dominant wave directions estimated from the radar data are consistent with the buoy results. Radar images present patterns of energetic components of ocean waves. For too-high and too-low ocean wave components, the radar is unable to image them effectively. This is attributable to the effects of radar imaging modulations. For longer wave patterns, the shadowed area affects the radar imaging of high-frequency waves; conversely, excessively short waves should be aliased after sampling by the pixel array. Based on the dispersion relation, the accuracies of estimated directional spectra at higher and lower frequency bins are also affected if simultaneous tide and current data are deficient. Based on our buoy observations, most mean wave periods at our study site are approximately within the range of 5-10 s. Thus, most of the energetic components of ocean waves are within this period range. Our comparison confirms that the dominant wave directions estimated from specified frequencies of radar directional spectra demonstrate better agreement with the buoy results, whose period is approximately equal to 5-10 s.

We also investigated the estimation of local wave directions in the spatial domain based on a highly inhomogeneous wave case. Although there are a few unreasonable wave directions, which are attributable to slightly unclear wave patterns in the radar image, most estimated wave directions demonstrate good agreement with the wave crest patterns. Local wave directions estimated from radar data represent the features of refracted waves. Therefore, we conclude that the analysis of simultaneous records of sea surface echo intensities from a selected marine radar image pixel array is an effective method for obtaining information on the wave directions in an inhomogeneous sea area.

ACKNOWLEDGMENT

The buoy data used in this study were measured and qualified by the Coastal Ocean Monitoring Center at the National Cheng Kung University. The radar images were provided by two engineers (Mr. Kun-I Lin and Mr. Tang-Chia Hsu) from the Taiwan Ocean Research Institute. The authors would like to express their sincere gratitude. In addition, the authors are grateful to the referees for helpful comments and suggestions.

REFERENCES

[1] M. Onorato *et al.*, "Statistical properties of directional ocean waves: The role of the modulational instability in the formation of extreme events," *Phys. Rev. Lett.*, vol. 102, no. 11, p. 114502, 2009.
[2] M. Benoit, P. Frigaard, and H. Schffer, "Analyzing multidirectional wave spectra: A tentative classification of available methods," in *Proc. IAHR Conf.*, San Francisco, CA, USA, 1997, pp. 131–158.
[3] R. Brockelman and T. Hagfors, "Note on the effect of shadowing on the backscattering of waves from a random rough surface," *IEEE Trans. Antennas Propag.*, vol. AP-14, no. 5, pp. 621–626, Sep. 1966.
[4] J. Wright, "Backscattering from capillary waves with application to sea clutter," *IEEE Trans. Antennas Propag.*, vol. AP-14, no. 6, pp. 749–754, Nov. 1966.
[5] S. S. Pawka, S. V. Hsiao, O. H. Shemdin, and D. L. Inman, "Comparisons between wave directional spectra from SAR and pressure sensor arrays," *J. Geophys. Res., Oceans*, vol. 85, no. C9, pp. 4987–4995, 1980.
[6] M. G. Mattie and D. L. Harris, "The use of imaging radar in studying ocean waves," in *Proc. 16th Conf. Coastal Eng.*, Hamburg, Germany, 1978, pp. 174–189.
[7] J. C. Nieto-Borge, K. Reichert, and J. Dittmer, "Use of nautical radar as a wave monitoring instrument," *Coastal Eng.*, vol. 37, nos. 3–4, pp. 331–342, Aug. 1999.
[8] V. Atanassov, W. Rosenthal, and F. Ziemer, "Removal of ambiguity of two-dimensional power spectra obtained by processing ship radar images of ocean waves," *J. Geophys. Res., Oceans*, vol. 90, no. C1, pp. 1061–1067, 1985.
[9] K. F. Hasselmann *et al.*, "The ERS SAR wave mode: A breakthrough in global ocean wave observations," ESA Special Publication 1326, 2013.

[10] W. Huang, X. Liu, and E. W. Gill, "Ocean wind and wave measurements using X-band marine radar: A comprehensive review," *Remote Sens.*, vol. 9, no. 12, p. 1261, 2017.
[11] J. C. Nieto-Borge and C. G. Soares, "Analysis of directional wave fields using X-band navigation radar," *Coastal Eng.*, vol. 40, no. 4, pp. 375–391, Jul. 2000.
[12] C. M. Senet, J. Seemann, S. Flampouris, and F. Ziemer, "Determination of bathymetric and current maps by the method DiSC based on the analysis of nautical X-band radar image sequences of the sea surface (November 2007)," *IEEE Trans. Geosci. Remote Sens.*, vol. 46, no. 8, pp. 2267–2279, Aug. 2008.
[13] K. Ma, X. Wu, X. Yue, L. Wang, and J. Liu, "Array beamforming algorithm for estimating waves and currents from marine X-band radar image sequences," *IEEE Trans. Geosci. Remote Sens.*, vol. 55, no. 3, pp. 1262–1272, Mar. 2017.
[14] N. N. Panicker and L. E. Borgman, "Directional spectra from wave-gage arrays," in *Proc. 12th Int. Conf. Coastal Eng.*, 2011, pp. 117–136.
[15] J. Yoo, "Nonlinear bathymetry inversion based on wave property estimation from nearshore video imagery," Ph.D dissertation, School Civil Environ. Eng., Georgia Inst. Technol., Atlanta, GA, USA, 2007.
[16] L.-C. Wu, L. Z.-H. Chuang, D.-J. Doong, and C. C. Kao, "Ocean remotely sensed image analysis using two-dimensional continuous wavelet transforms," *Int. J. Remote Sens.*, vol. 32, no. 23, pp. 8779–8798, 2011.
[17] J. Allender *et al.*, "The wadic project: A comprehensive field evaluation of directional wave instrumentation," *Ocean Eng.*, vol. 16, nos. 5–6, pp. 505–536, 1989.
[18] N. G. Plant, K. T. Holland, and M. C. Haller, "Ocean wavenumber estimation from wave-resolving time series imagery," *IEEE Trans. Geosci. Remote Sens.*, vol. 46, no. 9, pp. 2644–2658, Sep. 2008.
[19] R. Holman, N. Plant, and T. Holland, "cBathy: A robust algorithm for estimating nearshore bathymetry," *J. Geophys. Res., Oceans*, vol. 118, no. 5, pp. 2595–2609, 2013.
[20] P. L. F. Liu, *Advances in Coastal and Ocean Engineering*. Singapore: World Scientific, 1997.
[21] M. D. Earle, K. E. Steele, and D. W. C. Wang, "Use of advanced directional wave spectra analysis methods," *Ocean Eng.*, vol. 26, no. 12, pp. 1421–1434, 1999.
[22] R. A. Haubrich, "Array design," *Bull. Seismol. Soc. Amer.*, vol. 58, no. 3, pp. 977–991, 1968.
[23] Y. Goda, *Random Seas and Design of Maritime Structures*, 2nd ed. Singapore: World Scientific, 2000.
[24] A. D. Heathershaw, M. W. L. Blackley, and P. J. Hardcastle, "Wave direction estimates in coastal waters using radar," *Coastal Eng.*, vol. 3, pp. 249–267, Nov. 1979.
[25] L. H. Holthuijsen, *Waves in Oceanic And Coastal Waters*. Cambridge, U.K.: Cambridge Univ. Press, 2007.
[26] B. Lund, C. O. Collins, H. C. Graber, E. Terrill, and T. H. C. Herbers, "Marine radar ocean wave retrieval's dependency on range and azimuth," *Ocean Dyn.*, vol. 64, no. 7, pp. 999–1018, 2014.
[27] P. S. Bell, "Shallow water bathymetry derived from an analysis of X-band marine radar images of waves," *Coastal Eng.*, vol. 37, nos. 3–4, pp. 513–527, 1999.
[28] L.-C. Wu, D.-J. Doong, and J.-H. Wang, "Bathymetry determination from marine radar image sequences using the Hilbert transform," *IEEE Geosci. Remote Sens. Lett.*, vol. 14, no. 5, pp. 644–648, May 2017.

DONG-JIING DOONG received the Ph.D. degree from National Cheng Kung University (NCKU), Taiwan, in 2002. He is currently an Associate Professor with the Department of Hydraulic and Ocean Engineering, NCKU. His research interests include remote sensing techniques, ocean waves, and coastal hazards and protection.

LI-CHUNG WU received the Ph.D. degree in engineering from NCKU, Taiwan, in 2009. He has been an Assistant Research Fellow with the Coastal Ocean Monitoring Center, NCKU, since 2008. His research interests include remote sensing, ocean engineering, image processing, and wavelet transform.

JIAN-WU LAI received the Ph.D. degree in engineering from NCKU, Taiwan, in 2009. He has been an Associate Researcher with the Taiwan Ocean Research Institute, National Applied Research Laboratories, since 2014. His research interests include marine hydrodynamics and coastal process, ocean radar observing, and coastal disaster strategies.